JOURNAL OF SOLID STATE CHEMISTRY **134,** 376–381 (1997)
ARTICLE NO. SC977593

Synthesis, Resistivity, and Thermal Properties of the Cubic Perovskite $NH_2CH{=}NH_2SnI_3$ and Related Systems

D. B. Mitzi[1] and K. Liang

IBM T. J. Watson Research Center, P.O. Box 218, Yorktown Heights, New York 10598

Received May 19, 1997; in revised form August 8, 1997; accepted August 22, 1997

Combining concentrated hydriodic acid solutions of tin(II) iodide and formamidine acetate in an inert atmosphere results in the precipitation of a new conducting organic–inorganic compound, $NH_2CH{=}NH_2SnI_3$, which at room temperature adopts a cubic perovskite structure. The lattice constant for $NH_2CH{=}NH_2SnI_3$ is found to be $a = 6.316(1)$ Å, which is approximately 1.2% larger than that for the isostructural compound $CH_3NH_3SnI_3$. The electrical resistivity of a pressed pellet of the new compound exhibits semimetallic temperature dependence from 10 to 300 K, with evidence of a structural transition at approximately 75 K. $NH_2CH{=}NH_2SnI_3$ begins to slowly decompose in an inert atmosphere at temperatures as low as 200°C, with bulk decomposition/melting occurring above 300°C. The properties of the formamidinium-based perovskite are compared with those of the related cubic (at room temperature) perovskite $CH_3NH_3SnI_3$ and the mixed-cation system $(CH_3NH_3)_{1-x}(NH_2CH{=}NH_2)_xSnI_3$. © 1997 Academic Press

INTRODUCTION

While the majority of known halides are insulators, $CH_3NH_3SnI_3$ has recently been shown (1) to be a low carrier density p-type metal over the temperature range 2–300 K, with a small optical effective mass $m^* \approx 0.2$. This compound forms the basis for several more general structural families including $[NH_2C(I){=}NH_2]_2(CH_3NH_3)_mSn_mI_{3m+2}$, which consists of m-layer-thick $\langle 110 \rangle$-oriented $CH_3NH_3SnI_3$ perovskite slabs separated by layers of iodoformamidinium cations (2). Conduction occurs primarily along the perovskite slabs and a semiconductor–metal transition is observed as the perovskite sheet thickness is increased (i.e., larger m). A similar transition, as a function of increasing perovskite sheet thickness, has also been observed in the family $(C_4H_9NH_3)_2(CH_3NH_3)_{n-1}Sn_nI_{3n+1}$, which consists of $\langle 100 \rangle$-oriented perovskite slabs (3). In addition to conducting properties, the layered organic–inorganic perovskites exhibit a strong photoluminescence peak in the visible spectral range, with an emission wavelength that depends on the thickness of the perovskite sheets (4).

In contrast to the methylammonium cation, the solid-state chemistry of the formamidinium cation has not been extensively discussed in the literature. $[NH_2CH{=}NH_2]_3FeCl_6$ has been obtained, together with other products, from the reaction of S_4N_4 with HCl in CH_2Cl_2, in the presence of $FeCl_3$ (5). The solid-state structure consists of isolated $FeCl_6$ octahedra separated by two crystallographically independent formamidinium cations, one of which exhibits positional disorder. In another example, $[NH_2CH{=}NH_2]Zn(HCO_2)_3$, the formate ions link Zn atoms together in a three-dimensional network, with each Zn atom surrounded by six O atoms in approximately octahedral coordination. The formamidinium ions hydrogen bond through their N–H groups to adjacent formate groups (6). The Sn(IV) compound $[NH_2CH{=}NH_2]_2SnCl_6$ has also been made, although the structural details have not, to our knowledge, been reported (7).

In this work we discuss the synthesis and characterization of the Sn(II) compound $NH_2CH{=}NH_2SnI_3$, which like $CH_3NH_3SnI_3$ adopts a cubic perovskite structure at room temperature. A comparison between the new formamidinium compound and $CH_3NH_3SnI_3$ demonstrates a higher electrical resistivity in $NH_2CH{=}NH_2SnI_3$, as might be expected due to the expanded cubic lattice constant in this material. We also examine the possibility of making the solid solution $(CH_3NH_3)_{1-x}(NH_2CH{=}NH_2)_xSnI_3$, and demonstrate that the $x = 0.5$ member is isostructural with the $x = 0$ and $x = 1$ compounds, with a cubic lattice constant which is halfway between those of the two end members.

EXPERIMENTAL

1. Sample Preparation and Characterization

Polycrystalline $NH_2CH{=}NH_2SnI_3$ samples were prepared by precipitation from a hydriodic acid solution using

[1] To whom correspondence should be addressed.

0022-4596/97 $25.00
Copyright © 1997 by Academic Press
All rights of reproduction in any form reserved.

a procedure similar to that previously discussed for $CH_3NH_3SnI_3$ (1). Under flowing argon, tin(II) iodide (2.235 g, 6 mmol) was first dissolved at 70°C in 4 ml of a concentrated (57% by weight) aqueous HI solution. In a separate test tube, formamidine acetate (0.6246 g, 6 mmol) was dissolved at room temperature in 1.0 ml of concentrated aqueous hydriodic acid and immediately added to the tin(II) iodide solution (after allowing it to cool), leading to a thick black precipitate. Two additional 0.5-ml portions of hydriodic acid were used to rinse the formamidinium tube and were added to the test tube containing the product, which at all times was kept in an inert atmosphere of flowing argon. The product was maintained in the hydriodic acid solution for 15 min at room temperature, with periodic agitation of the solution, and filtered under flowing dry nitrogen gas. The yield was approximately 2.45 g (approximately 75% of the theoretical yield). The black powder was further dried under vacuum at room temperature and was subsequently stored and handled in an argon-filled glovebox, with oxygen and water levels maintained below 1 ppm.

Chemical analysis, performed by Galbraith Laboratories and averaged over six independent measurements, was consistent with the formula $NH_2CH{=}NH_2SnI_3$ (expected: C (2.21%), H (0.93%), N (5.14%); found: C (2.18%), H (0.95%), N (5.11%)). As seen in Fig. 1, infrared transmission spectroscopy, using pressed KBr pellets, yielded the following characteristic peaks (cm^{-1}): 595 (m), 1354 (m), 1630 (m), 1712 (s), and two broad regions of peaks (not well resolved), including approximately 3392 (m), 3340 (m), 3262 (m), and 3171 (w) and 1168 (m), 1121 (m), and 1045 (m). These frequencies are in reasonable agreement with those reported for the formamidinium cation in $[NH_2CH{=}NH_2]_3FeCl_6$ (5) and in $[NH_2CH{=}NH_2]_2SnCl_6$ (7). Of particular interest is the formamidinium C=N stretching vibration at 1712 cm^{-1}, which is shifted in the present compound (as well as in the two other examples listed) to higher frequency than typically observed for free amidines, presumably because of protonation (8).

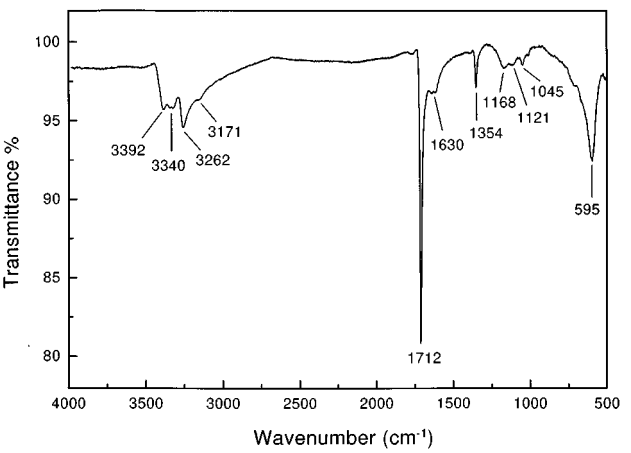

FIG. 1. Infrared transmission spectrum for $NH_2CH{=}NH_2SnI_3$, taken on a KBr pellet containing a small amount of the title compound. The numbers attached to the spectrum correspond to the major peak positions and have the units of cm^{-1}.

Samples of $CH_3NH_3SnI_3$ and the mixed-cation system $(CH_3NH_3)_{1-x}(NH_2CH{=}NH_2)_xSnI_3$ (with in this case $x = 0.5$) were synthesized in an identical fashion to that described for $NH_2CH{=}NH_2SnI_3$, except that a stoichiometric quantity of methylammonium iodide replaced formamidine acetate in the starting solution.

2. X-Ray Diffraction

Room temperature X-ray powder diffraction patterns were collected for each batch of samples, using a Siemens D5000 diffractometer (Cu$K\alpha$ radiation), and showed each product to be single phase. Indexing of the 19 diffraction peaks, over the range $10° \leq 2\theta \leq 80°$, was based on a comparison with a pattern from the isostructural $CH_3NH_3SnI_3$. The cubic unit cell dimensions were refined with the Siemens WIN-METRIC program (least-squares approach), after removing the $K\alpha_2$ component of the diffraction pattern and correcting for 2θ offset. For $NH_2CH{=}NH_2SnI_3$, the unit cell parameter obtained from the powder pattern, $a = 6.316(1)$ Å, agreed with that found from the single-crystal study (see later), while for $CH_3NH_3SnI_3$, the refined lattice parameter, $a = 6.242(1)$ Å, was consistent with our earlier study (1). For $(CH_3NH_3)_{0.5}(NH_2CH{=}NH_2)_{0.5}SnI_3$, refinement of the powder X-ray data yielded an intermediate lattice parameter value, $a = 6.278(1)$ Å, as would be expected for a solid solution of the two cations. No evidence of a superstructure, potentially arising from ordering of the organic cations in the structure, was found in the room temperature powder X-ray data.

In addition to the powder data, a $NH_2CH{=}NH_2SnI_3$ single crystal was examined using an Enraf-Nonius CAD4 diffractometer with graphite-monochromatized Mo$K\alpha$ (0.7107 Å) radiation. The unit cell parameters were obtained by a least-squares fit of 25 reflections with $20° \leq 2\theta \leq 32°$ and indicated a cubic cell with the lattice parameter $a = 6.312(1)$ Å.

3. Electrical Resistivity

Electrical resistivity measurements were performed in a displex system, using an airtight cell containing a four-point probe and a pressed pellet sample. The samples were pressed into 6-mm-diameter, approximately 1-mm-thick, circular pellets using 45,000 psi applied pressure. Given the chemical reactivity of the samples, electrical contacts were made using spring-activated pins directly contacting the sample. A contact resistance of approximately 1 Ω could be reproducibly achieved and maintained down to low temperatures. Resistivity measurements were taken at 1 K

intervals, during both warming and cooling, with the temperature being allowed to equilibrate at each step. At several points during the temperature scan, an I–V scan was taken to confirm the ohmic nature of the contacts. Copper and carbon standards, having the same geometry as the sample, were used to calibrate the resistance probe.

4. Thermal Analysis

Simultaneous thermogravimetric analysis (TGA) and differential thermal analysis (DTA) were performed, using a Seteram TAG 24 thermal analysis system, to examine the thermal stability and possible phase transitions of the title compound. Approximately 40–60 mg of sample was loaded into a tantalum container for each run, which consisted of a 2°C/min ramp from 20 to 370°C and back to 20°C in an argon atmosphere. Special care was taken to exclude oxygen from the apparatus by evacuating and back-filling the thermal analysis setup with argon. The temperature was calibrated using the melting transitions of indium ($T_m = 156.6$°C) and tin ($T_m = 231.9$°C) using the same system configuration (crucible type, temperature ramp rate, gas type, gas flow, etc.).

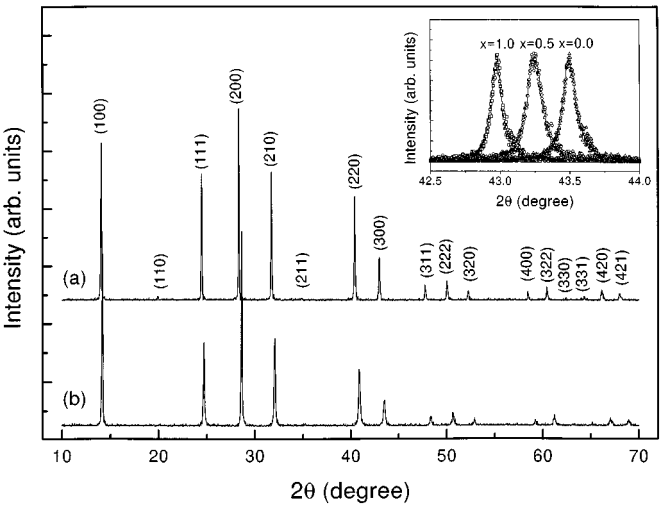

FIG. 2. Room temperature powder X-ray diffraction patterns for (a) $NH_2CH{=}NH_2SnI_3$ and (b) $CH_3NH_3SnI_3$. The pattern (not shown) for the mixed-cation system, $(CH_3NH_3)_{0.5}(NH_2CH{=}NH_2)_{0.5}SnI_3$, is intermediate to those for the two end-member compounds. The inset shows the (300) reflection for $(CH_3NH_3)_{1-x}(NH_2CH{=}NH_2)_xSnI_3$, with $x = 0$, 0.5, and 1.0, demonstrating the progressive shift in the cubic lattice constant across the series. In each of the diffraction patterns shown, the $K\alpha_2$ component has been stripped from the data.

RESULTS AND DISCUSSION

1. Structural Considerations

The cubic perovskite structures discussed in this work consist of a three-dimensional network of corner-shared $[SnI_6]^{4-}$ octahedra, with the organic cations located in the cuboctahedral cages formed by the 12 nearest-neighbor iodine atoms from the octahedra. Since the symmetries of the free organic molecules do not agree with the O_h site symmetry in the cubic perovskite structure, the methylammonium and formamidinium molecules must be orientationally disordered. In fact, for the isostructural cubic high-temperature phase of $CH_3NH_3PbX_3$ (X = Cl, Br, I), nuclear magnetic resonance (NMR) and nuclear quadrupole resonance (NQR) spectroscopies demonstrate that the $CH_3NH_3^+$ cations undergo rapid isotropic reorientation (9, 10). A similar situation is expected for the tin(II) iodide-based cubic perovskites.

Room temperature X-ray powder patterns for $NH_2CH{=}NH_2SnI_3$ (a) and $CH_3NH_3SnI_3$ (b) are shown in Fig. 2 and clearly demonstrate the isostructural relationship between the two compounds and the increase in the cubic lattice parameter when the smaller methylammonium cation is replaced with formamidinium. The progressive shift of the cubic lattice constant across the more complete series $(CH_3NH_3)_{1-x}(NH_2CH{=}NH_2)_xSnI_3$ ($x = 0.0$, 0.5, 1.0) is further highlighted in the inset to Fig. 2, which shows the (300) reflection for each of the three compounds. Notice that the (300) reflection for $x = 0.5$ is midway between the $x = 0$ and $x = 1$ reflections. In addition, this reflection is slightly broader than for the two end members (the peak FWHM is 0.13° for $x = 0.5$ vs 0.09° and 0.10° for the $x = 1.0$ and 0.0 samples, respectively), as might be expected due to the possibility of sample inhomogeneity for the solid solution sample. The peak width, however, can also vary with particle size, which depends on the precipitation process and the light grinding of the powders before X-ray analysis. Consequently, at this point, the small difference in peak width can only be considered suggestive.

In $NH_2CH{=}NH_2SnI_3$, the 3.158-Å Sn–I bond length (one-half of the cubic lattice parameter) is approximately 1.2% longer than in the metallic $CH_3NH_3SnI_3$ (3.121 Å). For comparison, the Sn–I bond distance for the high-temperature (black) cubic perovskite phase of $CsSnI_3$, which is also metallic, is 3.110 Å (11), again significantly shorter than in $NH_2CH{=}NH_2SnI_3$. The Sn–I bond length in the $x = 0.5$ compound, 3.139 Å, is halfway between the bond lengths observed in the $x = 1.0$ and $x = 0.0$ compounds.

Insulating tin(II) iodides tend to have longer Sn–I bond lengths and a tin(II) coordination which is highly distorted from a perfect octahedral arrangement. In the low-temperature (yellow) phase of $CsSnI_3$ (12), for example, the six Sn–I bonds range from 2.941 to 3.469 Å in length, with an average of 3.210 Å, while in the orange crystals of $[NH_2C(I){=}NH_2]_3SnI_5$, which exhibit a similar range of bond distances, the average Sn–I bond length is 3.202 Å (13). The SnI_6 octahedra in the yellow needlelike crystals of

$(CH_3)_2NH_2SnI_3$ are also highly distorted, with an average Sn–I bond length of 3.225 Å (14).

Semiconducting compounds tend to fall between the two extremes with respect to both bond length and degree of distortion of the SnI_6 octahedra. The darkly colored conducting layered perovskite $(C_4H_9NH_3)_2SnI_4$ has a slightly distorted octahedral tin(II) coordination, with bond lengths ranging from 3.133 to 3.160 Å and an average of 3.144 Å (15). Similarly, for $[NH_2C(I){=}NH_2]_2(CH_3NH_3)_2Sn_2I_8$, the Sn–I bond lengths range from 3.094 to 3.185 Å, and the average is 3.139 Å (2). It is interesting to note that while these average distances are longer than for the metallic cubic compounds $CsSnI_3$ and $CH_3NH_3SnI_3$, they are slightly shorter than for $NH_2CH{=}NH_2SnI_3$. In comparison with other refined tin(II) iodide-based structures then, the Sn–I bonds in $NH_2CH{=}NH_2SnI_3$ are somewhat long given that the structure exhibits an undistorted octahedral tin(II) coordination sphere and semimetallic conducting properties.

In fact, perfect octahedral coordination is uncommon in tin(II) chemistry. The most prevalent tin(II) coordination geometries are trigonal pyramidal and square pyramidal, both of which allow room for the Sn(II) lone pair of electrons, which can act as an extra ligand. The metallic tin(II) halide-based perovskites are unusual in that the Sn(II) lone pair is stereochemically inactive, enabling a perfect or slightly distorted octahedral coordination geometry. This and the shorter Sn–I bond lengths presumably arise in the more metallic systems because electron density from the Sn(II) lone pair states can delocalize into a conduction band (16). In addition to this electronic effect, however, there are clearly other factors, such as steric effects of the organic cation, which can influence the Sn–I bond length and the distortion of the coordination geometry. This steric effect presumably accounts for the longer Sn–I bond length in $NH_2CH{=}NH_2SnI_3$ (relative to $CH_3NH_3SnI_3$).

2. Electrical Transport

While the high-temperature phase for the $CH_3NH_3Pb\mathit{X}_3$ (X = Cl, Br, I) system is cubic and isostructural with the compounds considered in this work, upon cooling the structure distorts to lower symmetry as the motion of the methylammonium cation becomes more restricted. In contrast to the isotropic reorientation at high temperature, the lowest temperature phases for each of these systems is characterized by the organic cation being restricted to rotations about the C–N axis (9, 10). Similar structural transitions have been observed in $CH_3NH_3SnI_3$ and are likely as well in $NH_2CH{=}NH_2SnI_3$ upon cooling. Subtle changes in the slope of the resistivity as a function of temperature have been noticed in the system $CH_3NH_3SnI_3$ as a result of these structural transitions (1).

Figure 3a shows the resistivity of $NH_2CH{=}NH_2SnI_3$, as prepared in the experimental section, while the sample is being warmed from 10 to 300 K. Initially, the resistivity increases gradually with increasing temperature. At approximately 60 K, however, the resistivity rises sharply, reaching a peak at 75 K. Above 75 K, the resistivity decreases with increasing temperature, until around 200 K. Above this point, a small positive temperature derivative is again achieved, with a room temperature resistivity of order 10 mΩ-cm. Some hysteresis is noted in the transition at 75 K during warming and cooling (Fig. 3, inset), suggesting that the transition is first order. In analogy with $CH_3NH_3\mathit{M}I_3$ (M = Sn and Pb), the feature at 75 K is most likely an indication of a structural transition.

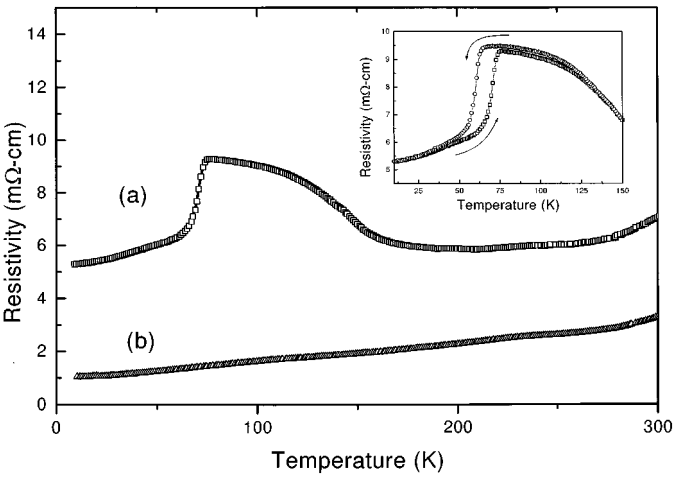

FIG. 3. Electrical resistivity measurements for pressed pellet samples of $(CH_3NH_3)_{1-x}(NH_2CH{=}NH_2)_xSnI_3$ with (a) $x = 1.0$ and (b) $x = 0.0$. Measurements were made using a four-point contact geometry. For clarity, only the warming curves are shown. The inset provides a more detailed look at the hysteresis in the low-temperature resistive transition, upon warming and cooling, for $NH_2CH{=}NH_2SnI_3$.

The resistivity curve for $CH_3NH_3SnI_3$ is also shown in Fig. 3 and has a positive temperature derivative over the entire temperature range. This compound has already been identified (1) as a low carrier density p-type metal, with a carrier density of approximately 2×10^{19} cm^{-3} (corresponding to only 0.005 holes per unit cell). It should be noted that the resistivity of the current $CH_3NH_3SnI_3$ sample is lower than that reported for the sample from our earlier study (1). In fact, the resistivity profile for $CH_3NH_3SnI_3$, and more generally for $(CH_3NH_3)_{1-x}(NH_2CH{=}NH_2)_xSnI_3$, is somewhat sensitive to the preparative conditions (solution temperature during precipitation, quality of the hydriodic acid used, whether the precipitate is recrystallized, etc.). Given the low carrier densities found in these materials, this variability can easily be accounted for by small numbers of vacancies or defects in the cubic perovskite structure on either the cation or anion site. Such vacancies are well known in other perovskite structures (17, 18). In addition, differences in the grain size within the pressed pellet samples

could also contribute to this batch-to-batch variability. In all cases examined, however, the resistivity values for $NH_2CH{=}NH_2SnI_3$ were larger than those in $CH_3NH_3SnI_3$ when the samples were prepared using the same technique.

The unusual electrical conductivity in each of these metal halide-based systems arises from the large dispersion of the Sn 5*s* band (hybridized with I 5*p*) along the $\langle 111 \rangle$ direction in the cubic Brillouin zone, leading to a marginal crossing of the Sn 5*s* and Sn 5*p* bands near the R point ($[\frac{1}{2}, \frac{1}{2}, \frac{1}{2}]2\pi/a$), with the Fermi energy falling roughly between the two bands (2). Presumably, the larger observed resistivity in the system $(CH_3NH_3)_{1-x}(NH_2CH{=}NH_2)_xSnI_3$, with $x = 1$ (relative to the $x = 0$ samples), is at least partially the result of the expansion of the cubic lattice, which leads to a narrowing of the bands and therefore a lower density of states at the Fermi energy. In addition, however, it is also possible that the substitution of the formamidinium cation for methylammonium might lead to a different preferred concentration of defects or vacancies in the structure as a result of the different molecular shape and functional groups. Small concentrations of such defects could readily produce a substantial shift in the already small carrier densities in these materials and therefore contribute to the observed difference in electrical transport behavior.

3. *Thermal Stability*

As a result of the organic cations in the title compounds, these materials are expected to decompose at relatively low temperatures. Figure 4 shows the thermal analysis curves for $NH_2CH{=}NH_2SnI_3$. The sample begins to slowly lose weight at temperatures as low as 200°C, but undergoes bulk decomposition/melting above 300°C. Upon heating the product of the 370°C thermal cycling a second time, there was little additional weight loss (approximately 1%) and a relatively sharp endotherm at 317(2)°C. This is in good agreement with the expected melting temperature for SnI_2 (320°C). In addition, the powder X-ray pattern for the product corresponded to SnI_2, verifying that this is in fact the final product of heating the material to 370°C in an inert atmosphere.

Note that the expected weight change, assuming the complete loss of $NH_2CH{=}NH_2I$ from the sample upon heating, would be 31.6%. As we observed a somewhat larger weight loss than this even during the first heating cycle, it is evident that some of the tin-containing intermediate and final products of the decomposition must also be volatile at the temperatures encountered during the thermogravimetric analysis scan. In fact, a SnI_2 sample subjected to the same thermal cycling to 370°C exhibited a weight loss of between 1 and 2%.

To further examine the mechanism of decomposition, chunks of $NH_2CH{=}NH_2SnI_3$ were placed in a sealed, evacuated, quartz tube and gradually heated in a temperature gradient until the sample (in the hottest section of the gradient) reached 220°C. After 1 week at 220°C, red needle-like crystals of SnI_2 were observed growing out of the chunks. The underlying black material, when X-rayed, revealed the same diffraction pattern as the starting cubic perovskite. Infrared spectra taken on this material also yielded a spectrum identical to that observed for the initial unheated sample. In addition to the red needles, there were also numerous clear crystals growing at the cool end of the quartz tube. These crystals had an infrared spectrum and X-ray diffraction pattern identical to those observed for NH_4I, indicating that the formamidinium cation had decomposed upon heating. The decomposition of $NH_2CH{=}NH_2SnI_3$ therefore does not simply proceed through the dissociation and loss of formamidine and hydrogen iodide from the sample, but rather also includes the pyrolysis of formamidine to form (among other products) ammonia.

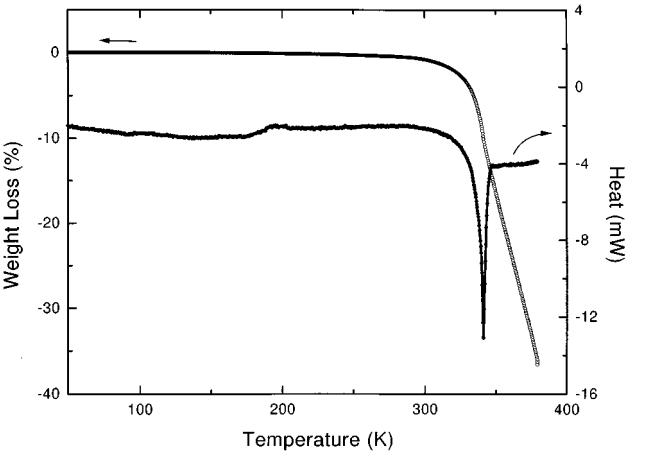

FIG. 4. Simultaneous thermogravimetric analysis and differential thermal analysis scans for $NH_2CH{=}NH_2SnI_3$. The measurement was made in an argon atmosphere using a 2°C/min heating rate. For clarity, only the heating segment is shown.

CONCLUSIONS

The perovskites $(CH_3NH_3)_{1-x}(NH_2CH{=}NH_2)_xSnI_3$ ($x = 0.0$, 0.5, 1.0) have all been shown to adopt a cubic perovskite structure at room temperature. With increasing x, the lattice parameter increases from $a = 6.242$ Å ($x = 0$) to $a = 6.316$ Å for ($x = 1$). The fact that the lattice constant of the $x = 0.5$ compound is intermediate to those of the two end members demonstrates that a solid solution of the two cations can be formed. The shift in lattice constant in going from $x = 1$ to $x = 0$ is analogous to applying hydrostatic pressure and provides the ability to study the properties of the tin(II) iodide-based cubic perovskite structure as a function of "chemical pressure"or lattice constant.

While each of the members in the series $(CH_3NH_3)_{1-x}(NH_2CH{=}NH_2)_xSnI_3$ ($x = 0.0$, 0.5, 1.0) is cubic at room temperature (with a necessarily disordered organic cation), a lowering of symmetry is expected at lower temperature as a result of organic cation ordering. A relatively sharp transition in the resistivity of $NH_2CH{=}NH_2SnI_3$ at approximately 75 K suggests that a structural transition occurs for $x = 1$ near liquid nitrogen temperature. While analogous structural transitions have been reported in $CH_3NH_3SnI_3$ (1) and $CH_3NH_3PbX_3$ (X = Cl, Br, I) (9, 10), the formamidinium system is particularly interesting since it has an extra NH_2 group, which lengthens the molecule and provides an additional site for hydrogen bonding, thereby presumably enhancing the tendency for ordering. The systems with $0 < x < 1$ are also very interesting since these contain a mixture of organic cations with two and three heavy atoms. A study of how the cation ordering is affected by this mixing is an area of further interest for this system.

Finally, $[NH_2C(I){=}NH_2]_2(CH_3NH_3)_mSn_mI_{3m+2}$ (2) and $(C_4H_9NH_3)_2(CH_3NH_3)_{n-1}Sn_nI_{3n+1}$ (3) are two examples of lower dimensional perovskite families based on $CH_3NH_3SnI_3$ with interesting physical properties that can be tailored by increasing the perovskite sheet thickness (varying m or n), changing the distance between the perovskite sheets (replacing butylammonium with other longer or shorter organic ammonium cations), or changing the band gap of the inorganic layers (by, for example, replacing tin(II) with lead(II) or germanium(II)) (15). $CsSnI_3$, which forms a cubic perovskite structure at high temperature, similarly can be used to generate a series of layered perovskites (19). In analogy with these two systems, $NH_2CH{=}NH_2SnI_3$ may also form the basis for a series of lower dimensional perovskites with interesting conducting and luminescent properties. The ability to substitute this cation into the lower dimensional structures is expected to provide an additional degree of "band gap engineering" in these materials.

ACKNOWLEDGMENT

The authors gratefully acknowledge ARPA for partial support of this work under Contract DAAL01-96-C-0095.

REFERENCES

1. D. B. Mitzi, C. A. Feild, Z. Schlesinger, and R. B. Laibowitz, *J. Solid State Chem.* **114,** 159 (1995).
2. D. B. Mitzi, S. Wang, C. A. Feild, C. A. Chess, and A. M. Guloy, *Science* **267,** 1473 (1995).
3. D. B. Mitzi, C. A. Feild, W. T. A. Harrison, and A. M. Guloy, *Nature* **369,** 467 (1994).
4. G. C. Papavassiliou and I. B. Koutselas, *Synth. Met.* **71,** 1713 (1995).
5. U. Demant, E. Conradi, U. Müller, and K. Dehnicke, *Z. Naturforsch., B* **40,** 443 (1985).
6. R. E. Marsh, *Acta Crystallogr., C* **42,** 1327 (1986).
7. M. Kuhn and R. Mecke, *Chem. Ber.* **94,** 3016 (1961).
8. L. J. Bellamy, "The Infra-red Spectra of Complex Molecules," pp. 299–303. Chapman and Hall, New York, 1975.
9. Q. Xu, T. Eguchi, H. Nakayama, N. Nakamura, and M. Kishita, *Z. Naturforsch. A* **46,** 240 (1991).
10. R. E. Wasylishen, O. Knop, and J. B. Macdonald, *Solid State Commun.* **56,** 581 (1985).
11. K. Yamada, S. Funabiki, H. Horimoto, T. Matsui, T. Okuda, and S. Ichiba, *Chem. Lett.* 801 (1991).
12. P. Mauersberger and F. Huber, *Acta Crystallogr., B* **36,** 683 (1980).
13. S. Wang, D. B. Mitzi, C. A. Feild, and A. Guloy, *J. Am. Chem. Soc.* **117,** 5297 (1995).
14. G. Thiele and B. R. Serr, *Z. Kristallogr.* **211,** 48 (1996).
15. D. B. Mitzi, *Chem. Mater.* **8,** 791 (1996).
16. J. D. Donaldson and S. M. Grimes, *Rev. Silicon, Germanium, Tin, Lead Compd.* **8,** 1 (1984).
17. C. Michel and B. Raveau, *Rev. Chim. Miner.* **21,** 407 (1984).
18. F. Galasso, "Structure, Properties and Preparation of Perovskite-Type Compounds," pp. 10–11. Pergamon Press, New York, 1969.
19. D. B. Mitzi, *Bull. Am. Phys. Soc.* **38,** 116 (1993).